[11] High-Resolution, High-Throughput Microscopy Analyses of Nuclear Receptor and Coregulator Function

By VALERIA BERNO,* CRUZ A. HINOJOS,* LARBI AMAZIT, ADAM T. SZAFRAN, and MICHAEL A. MANCINI

Abstract

Steroid nuclear receptors are ligand-dependent transcription factors that have been studied since the early 1960s by principally biochemical and reporter assay approaches. From these studies an elegant and complex model of nuclear receptor transcription regulation has been developed. Inherent to both biochemical and reporter assay approaches is the generation of averaged responses and it is not generally considered that individual cells could exhibit quite varied responses. In some cases, recent microscopic single-cell analyses provide markedly different responses relative to traditional approaches based on population averaging and underscore the need to continue refinement of the current model of nuclear receptor-regulated transcription. While single-cell analyses of nuclear receptor action have been hindered by the predominantly qualitative nature of the approach, high-throughput microscopy is now available to resolve this issue. This chapter demonstrates the utility of high-throughput microscopic analyses of nuclear receptor and nuclear receptor coregulator function. The ability of high-throughput microscopy to generate physiologically appropriate test populations by filtering based on morphological and protein of interest expression criteria is demonstrated. High-resolution, high-throughput microscopy is illustrated that provides quantitative subcellular information for both androgen and estrogen receptors. Efforts are ongoing to develop model systems that provide additional multiplex data and with refined image analyses to achieve true high-content imaging screens.

High-Throughput Microscopy (HTM)

High-throughput microscopy for biological purposes may be broadly defined as an automated image acquisition system coupled to cell identification and cell morphological detection/measurement algorithms. Automated image acquisition and the multiple aspects of cellular and subcellular morphology measured and catalogued at the individual cell level enable the potential generation of millions of measurements per day and impart the

*Primary contributors.

METHODS IN ENZYMOLOGY, VOL. 414

0076-6879/06 $35.00
DOI: 10.1016/S0076-6879(06)14011-2

high-information content inherent to this methodology. A significant benefit of the morphological measurements is the ability to filter (or gate) the imaged cell population to obtain a more homogeneous subpopulation for analysis. For example, apoptotic and mitotic cells may be morphologically identified and excluded from the final population to be analyzed. The ability to filter cells is especially beneficial when studying exogenously expressed proteins by allowing the exclusion of cells that are over- or underexpressing the protein relative to the endogenous level. Further, the numerous measurements enable the multiplexing of numerous morphological features in order to rapidly identify correlations and underscore the large analytical potential of HTM (Perlman *et al.*, 2004).

Technological innovations continue to improve HTM as developers advance imaging systems, design specialized algorithms to measure specific subcellular phenomena, and create more intuitive and comprehensive software tools for data mining. For example, algorithms were developed that specifically measure the fractional localization of a protein between the cytoplasm and the nucleus. These algorithms were applied to quantitate the cytoplasmic to nuclear translocation of the transcription factor NF-κB–p65 subunit upon proinflammatory cytokine stimulation by two separate HTM systems (Ding *et al.*, 1998; Morelock *et al.*, 2005). The successful matching of NF-κB biology with proper analytical tools was an early and highly extrapolatable HTM analysis tool that formed the basis of many translocation assays. Successful HTM analysis is therefore predicated upon utilizing or developing appropriate model systems.

Steroid Nuclear Receptors and Coregulators

Steroids are secreted endocrine hormones that are involved in a broad range of physiological functions such as sexual differentiation, growth and development, metabolism, and maintenance of homeostasis. In response to trophic signals, the adrenal glands (cortisol and aldosterone producing) or gonads (progesterone, testosterone, and estradiol producing) secrete steroids into the blood stream (Singh and Kumar, 2005). Steroid signals are transduced through binding to steroid nuclear receptors (NR). NRs are a family of transcription factors that include androgen (AR), estrogen (α and β isotypes, ERα and ERβ), glucocorticoid (GR), progesterone (A and B isoforms, PRA and PRB), and mineralocorticoid receptors (Evans, 1988). Steroid binding to these receptors affects transcription regulation of specific genes. Thus, steroids play a key role in the development or maintenance of multiple physiological phenotypes by altering transcription through NRs; not surprisingly, aberrant regulation of steroid signaling may result in pathophysiological conditions. The Nuclear Receptor Signaling Atlas (www.nursa.org) is a useful online resource for the entire NR community.

Nuclear receptors share common structural domains that are critical for the regulation of transcription (Kumar and Thompson, 1999). These domains include the DNA-binding domain (DBD), the ligand-binding domain (LBD), and activation functions 1 and 2 domains (AF-1, AF-2). Binding of ligand to the LBD causes a conformational change that promotes DNA promoter binding through the DBD. The receptor interacts as a dimer with DBD-specific hormone response elements to either inhibit or promote transcription of a set of responsive genes through the recruitment of coregulators. In the inactive or repressed state, the promoter-localized NR directly or indirectly recruits corepressor proteins such as histone deacetylases and other nuclear receptor corepressors. These proteins generate a transcriptionally prohibitive environment through histone modifications (e.g., acetylation, methylation) and chromatin condensation. Alternatively, binding of agonist to the NR reduces the association with corepressor proteins and increases the recruitment of multiple coactivator proteins such as steroid receptor coactivators (SRC-1, -2, and -3), chromatin-remodeling proteins, basal transcription factors, and RNA pol II. Specificity is generated by (1) the functional redundancy of many of the coregulators, resulting in an exponential number of protein combinations within a complex; (2) promoter-specific recruitment of coregulators; and (3) modulation of coregulators by signal transduction pathways. Thus, transcription is regulated through the NR and ligand-dependent recruitment to promoters of functionally distinct proteins.

Nuclear receptors each have unique properties that either lend to or detract from HTM analysis. The subcellular localization of each NR is a critical feature in any imaging assay. The AR, GR, MR, and PR members of the NR family are principally located in the cytoplasm in the absence of their ligands. Here, the nonliganded NR associates with chaperone proteins, such as heat-shock protein 90 (Pratt *et al.*, 2004). Addition of ligand induces NR homodimerization and a cytoplasm to nuclear translocation facilitated by dynamic interactions with chaperone proteins to the liganded receptor. The cytoplasmic NR translocation to the nucleus is analogous to NFκB translocation and is, therefore, conducive for study by existing HTM capabilities. Therefore, novel NR ligands may be screened and analyzed by HTM for their ability to induce NR cytoplasm to nuclear translocation (see later). In contrast, the ER and PRA are principally localized to the nucleus in the absence of ligand preventing HTM analysis of translocation (Press *et al.*, 1989; Lim *et al.*, 1999), although one could envision screens to examine effectors that lead redistribution to the cytoplasm. For nuclear resident proteins, novel HTM methods and model systems are required to study functional responses to ligand (see later).

We have adopted HTM as an analytical tool to study steroid nuclear receptor and nuclear receptor coregulator biology at the single-cell level. The critical aspects of experimental setup necessary for successful and reliable HTM analysis of AR and ER and one NR coregulator, SRC-3, are discussed. Each protein has distinct properties that require different model systems and application of HTM for analysis. The following sections describe these model systems, their analyses by HTM, and representative results.

General Methods

Cover Glass Preparation

Acid Etching Coverslips. Within a fume hood, heat coverslips in a loosely covered glass beaker (can use foil) in 1 *M* HCl at 50 to 60° for 4 to 16 h. An entire box of coverslips may be processed at once. Next pour off and save the acid and wash the coverslips extensively with sterile dH_2O. At this point, the coverslips may be rinsed with ethanol and laid out separately and left to dry on a sheet of 3MM paper under ultraviolet light. When dry, place the coverslips in a sterile culture dish for storage. We use 12-mm circular coverslips, which are conveniently sized for 24-well cell culture plates for growth and processing.

Coating with Poly-D-Lysine

Some cells do not adhere well to acid-etched cover slips and require an additional treatment. We coat acid-washed cover slips with poly-D-lysine; this can also be done in bulk using 100-mm cell culture dishes. If an entire box of coverslips is to be coated, divide them among four dishes. Prepare 1 mg/ml poly-D-lysine, reconstituted in sterile phosphate-buffered salilne (PBS), and filter sterilize (use a 10-ml syringe and syringe filter). Use about 10 ml per dish, sealing the dishes with Parafilm. One dish at a time may be coated and the poly-D-lysine transferred to the next dish when the first one is finished, and so on. Rock or rotate the dishes a minimum of 30 min. Remove and save the poly-D-lysine; it can be reused three or four times if refiltered and stored at −20°. Wash the coverslips with sterile dH_2O a minimum of five times in order to completely remove leftover poly-D-lysine. Next, rinse with ethanol, separate, and store as described in the acid-washing section. The coated coverslips may also be stored in ethanol, sealing the dishes with Parafilm until separating.

For glass-bottom well plates we also coat with poly-D-lysine or hormone-free stripped-dialyzed fetal bovine serum. The protocol for acid

etching and poly-D-lysine coating well plates is similar to that of coverslips. The differences are that the acid etching should occur for a maximum of 4 h at 50° in order to minimize damage to the adhesive present in the plate. Care should also be taken not to let the poly-D-lysine dry within the well as this will cause an uneven surface for the cells to grow upon. Alternatively, the glass-bottom plates may be coated with stripped-dialyzed serum overnight at 37° within a cell culture incubator in order to prevent drying of the serum onto the cover glass. After incubation, the excess serum is removed; the plates are ready to be seeded with cells.

Cell Culture and Experimental Setup

Grow cells in the appropriate growth media and serum (usually 5% fetal bovine serum) to 90 to 95% confluency. Refresh the growth media 1 day prior to subculturing the cells onto coverslips or well plates following standard trypsin digestion protocols. For NR experiments, the subcultured cells are grown in medium that contains stripped and dialyzed serum that lacks hormones that can obfuscate results. The appropriate seeding density is dependent on many factors and must be determined empirically for each experiment (see specific examples). The cells are grown for 24 to 48 h on the cover glass until ligand treatment or transfection of expression vector(s).

DNA Transfection

Perform transfections by standard calcium phosphate precipitation protocols or by commercially available lipid-based transfection reagents following the manufacturer's protocol. If cells are not to be transfected then perform the ligand treatments and proceed to the fixation and immunolabeling protocol. Remove the medium containing the transfection reagent and expression vector and replace with medium containing the appropriate ligand and control treatments. In our experience, empirically evaluating a variety of transfection reagents and protocols is required for optimal results, which can be significantly cell line specific.

Formaldehyde Fixation and Immunolabeling of Cells

Antibody labeling of endogenous proteins must be optimized to achieve maximal signal-to-noise levels of the fluorescent signals. For cells expressing fluorescent protein fusions, the signal can be increased by immunolabeling the fluorescent protein and/or the protein of interest. For example, cells expressing green fluorescent protein (GFP) fused to the estrogen receptor (GFP-ERα) can be labeled using an ERα antibody or GFP antibody and a green fluorescing secondary antibody. We have found that double labeling can decrease the exposure time manyfold.

Initial Fixation

1. Remove culture media by aspiration or pipetting. Wash cells one to two times with ice-cold PBS (Ca^{2+} and Mg^{2+} containing).
2. Remove PBS and fix the cells with 4% formaldehyde on ice for 30 min.
3. Remove formaldehyde fix, discard in toxic waste bottle, and wash three times with PEM buffer, about 1 to 5 min per wash.
4. Quench autofluorescence: add PEM buffer to preweighed sodium borohydride (final concentration of 1 mg/ml). Mix and add to coverslips. Incubate for 5 min at room temperature, replace with fresh PEM/$NaBH_4$, and incubate another 5 min. Check coverslips to make sure they are not floating on top of the buffer due to the expected bubbling action generated. Alternatively, add 100 m*M* of ammonium chloride for 10 min at room temperature.
5. Wash with PEM twice, 5 min each time.
6. Permeabilize cell membranes: incubate cells at room temperature 30 min with PEM containing 0.5% Triton X-100. The amount of time in detergent is generally antigen/antibody specific; ~5 min is sometimes sufficient, but to ensure full penetration of antibodies into dense chromatin, we have found 30 min is required.
7. Wash three times with PEM, about 1 to 5 min per wash. If immunolabeling, wash once with Tris-buffered saline plus Tween 20 (TBS-T) buffer after the PEM washes.

Note: If working with cells that are not going to be immunolabeled (such as cells expressing XFP-fused proteins), proceed to the 4′,6-diamidino-2-phenylindole (DAPI) counterstaining step. Instead of using TBS-T, you may dilute the DAPI in PEM to 1 μg/ml working concentation. Incubate with DAPI a minimum of 3 min; again, this should be determined empirically for different cell lines.

Immunolabeling

1. Block nonspecific binding sites with 5% nonfat powdered milk in TBS-T buffer plus 0.02% sodium azide. Blocking time can be anywhere from 30 min to 1 h at room temperature or overnight at 4°. One percent bovine serum albumin in TBS-T can be substituted for powdered milk.
2. Remove blocking buffer and add primary antibody diluted in blocking buffer. Incubate 30 min at 37°, 1 to 2 h at room temperature, or overnight at 4°.
3. Remove primary antibody (generally, the primary antibody can be saved, frozen, and reused several times). Wash four to five times with blocking buffer, 1 min or more per wash.
4. Add fluorochrome-coupled secondary antibody diluted in blocking buffer. Incubate 30 min at room temperature protected from light. We

have found the Alexa dyes from Molecular Probes to be outstanding in terms of brightness and stability (www.probes.com). We routinely dilute the secondary antibodies manyfold more than recommended. Remove and save secondary antibody as it also can be reused. Wash five times with TBS-T and then wash with PEM.

Postfixation and Quenching

As high-magnification, high-resolution imaging systems became more sensitive, we found that antibody-labeled proteins sometimes exhibited minor movements, even through the eyepiece (at 100×). Presumably this was due to partial unfixing from formaldehyde cross-linking and could cause some blurriness in the images. Thus, we began introducting a post-fixation step to ensure stabilization of the antigen–antibody complexes for high-resolution work or, importantly, for longer-term storage of slides (weeks at 4°).

Note: The cells now need to be shielded from light.

1. Fix 10 to 30 min in 4% formaldehyde in PEM buffer.
2. Remove fix (discard in toxic waste) and wash three times in PEM, 2–5 min per wash.
3. Quench autofluorescence as described initially.
4. Wash with PEM twice, 5 min each time.
5. Wash two to three times with TBS-T.
6. Counterstain DNA with 1 μg/ml of DAPI diluted in TBS-T for a minimum of 3 min. Note: DAPI staining is a critical step in achieving successful HTM imaging. For imaging systems that do not use reflection of cell substratum, for example, focusing on the cells directly, a bright high-contrast DAPI stain of nuclei is necessary and is inherently useful in subsequent cell identification. Hoeschst or other DNA stains may also be used.
7. Remove DAPI and add TBS-T.
8. Mount the coverslips on the slide with an antifade mounting medium and seal with nail polish if necessary. For well plates add weak fixative (PEM or PBS and 0.4% formaldehyde) and store at 4° until imaging. Because formaldehyde is autofluorescent, the weak fixative must be replaced with either PEM or PBS buffer prior to imaging. We have found that the newly released Slow Fade or Prolong ''Gold'' from Molecular Probes is particularly useful to prevent photobleaching, especially in the green and red channels.

Reagents and Supplies

- PBS containing Ca^{2+} and Mg^{2+} (PBS) and TBS-T buffers: formulations of these buffers can be found in common protocol books.

- PEM buffer: 80 m*M* potassium PIPES, pH 6.8, 5 m*M* EGTA, pH 7.0, and 2 m*M* $MgCl_2$.

Filter sterilize and store at 4°.

- Formaldehyde: Use EM-grade formaldehyde (stock solutions range from 16 to 20% and are provided in glass ampoules). Working solution is 4% formaldehyde diluted in PEM buffer. Cover opened ampoules with Parafilm and store at 4°. We abandoned preparation of our own formaldehyde from paraformaldehyde powder to improve fixation consistency and for safety consideration.
- Triton X-100: For ease of use, make a 10% weight/volume stock solution of the Triton X-100 in PEM buffer and aliquot to microcentrifuge tubes covered with foil or amber-colored tubes to protect from light. Store the stocks at −20°. The working solution is 0.5% Triton X-100 diluted in PEM buffer. Diluted Triton is unstable. Do not refreeze the aliquots (store in a refrigerator a maximum of 1 week).
- DAPI: Make a 1-mg/ml stock solution in PEM buffer and aliquot to microcentrifuge tubes covered with foil or amber-colored tubes to protect from light. Store at 4°.

Imaging

High-resolution HTM analyses for all studies described are performed using the Cell Lab IC 100 Image Cytometer (IC100) platform and Cytoshop Version 2.1 analysis software (Beckman Coulter). The imaging platform consists of (1) Nikon Eclipse TE2000-U inverted microscope (Nikon; Melville, NY) with Chroma 82000 triple band filter set (Chroma; Brattleboro, VT), (2) Hamamatsu ORCA-ER digital CCD camera (Hamamatus; Bridgewater, NJ), and (3) Photonics COHU progressive scan camera (Photonics; Oxford, MA). The objective used is a Nikon S Fluor 40×/0.90NA. The objective is chosen as the minimum required to obtain subcellular resolution. The 12-bit images are generated with 1 × 1 binning (1344 × 1024 pixels; 6.5 μm^2 pixel size).

Nuclear Receptor Coregulator SRC-3

The nuclear receptor coactivator SRC-3 belongs to the p160/SRC (steroid receptor activator) family that also includes SRC-1 and SRC-2 (McKenna *et al*., 1999). Members of this family directly bind to nuclear receptors and are intricately involved in receptor regulation. SRCs assist in activating transcription through their two transcription activation domains as well as acting as a scaffold for other transcription-related proteins.

SRC-3 is strongly suggested to play an oncogenic role in cancer: the SRC-3 gene is amplified in ~10% of human breast cancers, and SRC-3 mRNA and protein expression are elevated in a majority of tumors. *In vivo* mouse studies also show that overexpression of SRC-3 alone is sufficient to initiate tumorigenesis. At the subcellular level, the majority of SRC-3 is localized within the nucleus but translocates rapidly between the nucleus and the cytoplasm (Amazit *et al*., 2003). At the molecular level, SRC-3 contains several serine/threonine phosphorylation sites. Standard reporter assays show that phosphorylation of SRC-3 regulates its transcription activity (Wu *et al*., 2005). The ability of HTM and single-cell analysis to generate a more homogeneous and physiologically appropriate cell population for the study of subcellular phenomena is a great advantage over traditional reporter and biochemical assays. HTM will allow for the study of SRC-3 phosphorylation in regulating its subcellular distribution, cyto/nuclear shuttling, and interaction with transcription proteins at visible promoter arrays. To analyze SRC-3 by single-cell, microscopy techniques rapidly, the protein and its phosphorylation mutant variants are fused with green fluorescent protein and transiently expressed in tissue culture cell lines. In experiments with transiently expressed SRC-3 and, in general, all exogenously expressed proteins, we find that it is imperative to select cells that have near-endogenous levels of expression in order to evaluate natural functions. This section describes how to use HTM to properly select cells for analysis based on cell viability and expression of exogenous SRC-3.

Protein Expression Level Assay

Experimental Setup

Cell Culture, Treatment, and Labeling. Cell culture and transfection of HeLa cells are performed as described in earlier. Cells may be grown on either coverslips or glass-bottom well plates. Particular to SRC-3, optimal expression time posttransfection for pEGFP-SRC-3 expression vector has been determined to be 48 h and the cell density at the time of fixation is 50 to 70%. In addition, HeLa cells are mock transfected in parallel to pEGFP-SRC-3 transfection. After fixation both mock transfected and transfected cells are immunolabeled for SRC-3 as described earlier. The secondary antibody is conjugated to Alexa 555 (Molecular Probes).

Imaging, Data Extraction and Filtering, and Data Analysis. Both pEGFP-SRC-3-transfected and mock-transfected cells are imaged using the 40×/0.90 NA high-resolution objective. The 40× objective is chosen,

in part, based on the balance between field size (number of cells imaged) and resolution. The high resolution will be required in subsequent studies to allow observation of subnuclear patterns such as the nuclear speckling associated with transcriptionally active SRC-3, as well as the androgen and estrogen receptors. The mock-transfected cells (containing only endogenous SRC-3) are imaged for DAPI and red immunofluorescence. The pEGFP-SRC-3-transfected cells are imaged for DAPI, red immunofluorescence, and GFP, maintaining the same exposure time for the red channel.

Cells are identified and extracted by generating nuclear area masks using a nonlinear least-squares optimized image filter to create marked object–background contrast, followed by automatic histogram-based thresholding. Estimating and subtracting the mean background image intensity, determined dynamically on a per-image basis, correct effects due to background fluorescence. The correlated channel mask is computed as an intersection between the threshold correlated channel image (the threshold level is computed dynamically using a proprietary background level estimation method, Beckman Coulter), a Voroni tessellation polygon, and a circle of user-defined radius from the nuclear centroid. The resulting imaged cell population is biologically heterogeneous (Fig. 1A).

Threshold filters standard to Cytoshop are applied to increase the homogeneity of the imaged cell population by removing aberrant cells. Three filters are applied simultaneously to the total imaged cell population:

1. DNA content outlier: removes apoptotic and mitotic cells based on DAPI intensity (Fig. 1B)
2. DNA cluster: removes cell clusters that could not be resolved as individual cells (Fig. 1B).
3. Cells acquired with two channels: removes cells that do not contain data for at least two user-defined channels (Fig. 1B). Filter application to the mock-transfected and GFP-SRC-3 expressing imaged cell populations produces morphologically homogeneous and viable interphase cell subpopulations (Fig. 1B).

Examination of the mean nuclear fluorescence of endogenous (red channel) SRC-3 in mock-transfected cells indicates a broad range of expression (Fig. 2A). Similar examination (red channel) of GFP-SRC-3 expressing cells indicates a higher maximal range of expression as expected. Also, overexpression of SRC-3 causes the formation of nonphysiological globules (or aggregates, foci, etc.) of the SRC-3 protein (Fig. 2B). To minimize total SRC-3 overexpression artifacts, the maximum expression in GFP-SRC-3 expressing cells is conservatively set to three times the

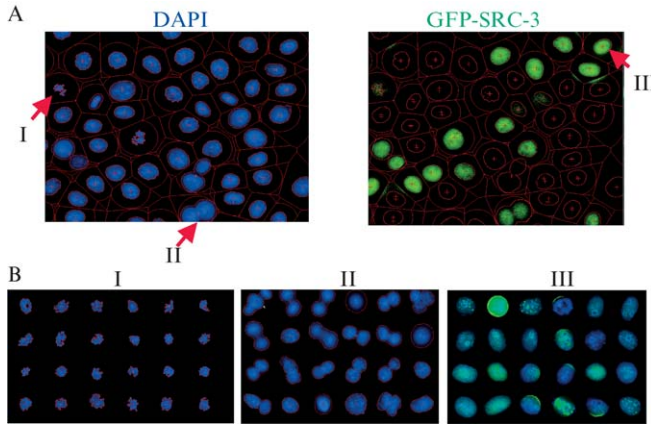

FIG. 1. Morphological filtering of total imaged cell population. Two channels are imaged in a single plane using a 40×/0.90 NA objective: channel 0 (DAPI) and channel 1 (pEGFP-SRC-3). (A) A representative field of Hela cells transiently expressing GFP-SRC-3 is presented. Contrast measurements identify DAPI-stained nuclei and Voroni tessellation polygons (red boundaries) define the cell boundaries. Present within this field are (I) apoptotic or mitotic cells, (II) unresolved nuclei clusters, and (III) interphase cells differentially expressing GFP-SRC-3. (B) Galleries of I, II, and III cells are presented. For gallery I, a DNA content algorithm is applied to identify the apoptotic and mitotic cells. For gallery II, a DNA cluster algorithm is applied to identify the clusters of nonresolved nuclei. Keep cells with two channels filter are combined with the previous filters and applied to the total cell population to generate a more homogeneous population (gallery III) of interphase cells differentially expressing GFP-SRC-3.

maximum expression found in mock-transfected cells. The corresponding fluorescence value in the green channel is identified and used as the maximum fluorescence value in a custom filter for GFP-SRC-3 expressing cells not immunolabeled and used for subsequent cell filtering (Fig. 2C). All cells within this range do not exhibit SRC-3 globule formation; importantly, antibody labeling of SRC-3 (and SRC-1 and SRC-2, data not shown) also fail to show large intranuclear foci. It is important to note that the expression range values are not absolute and differ between experiments due to biological, experimental, and optical variability.

Androgen Receptor

This section discusses the HTM procedure for studying translocation and nuclear distribution of one specific NR, the androgen receptor. The main function of androgenic signaling is male sex differentiation, pubertal

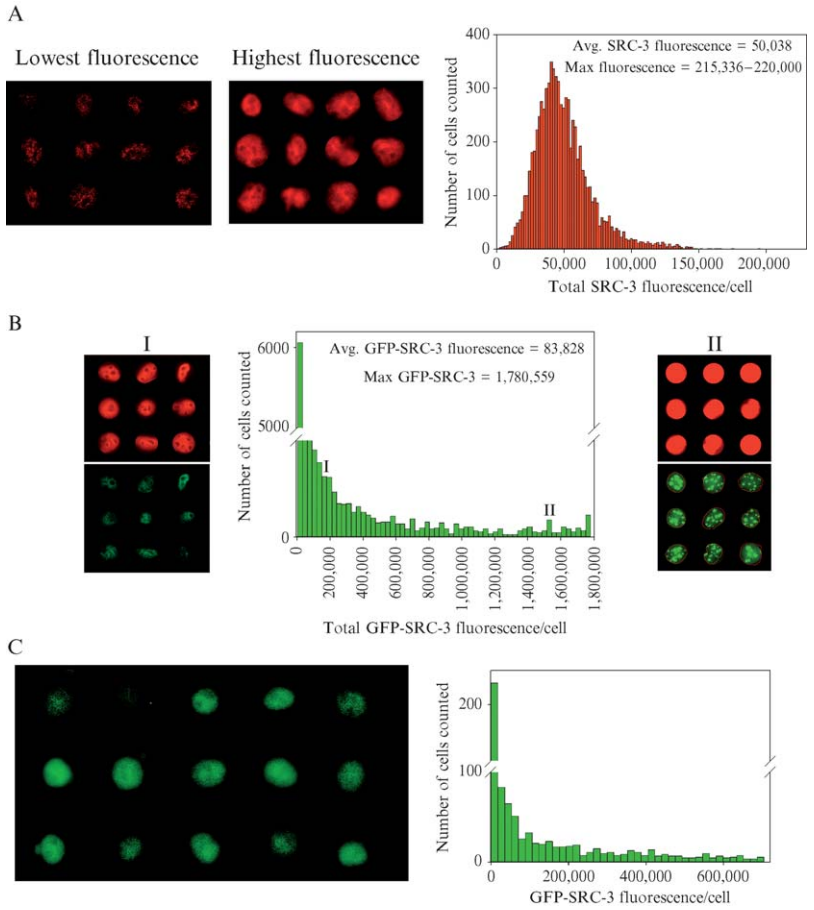

FIG. 2. Selecting cells expressing SRC-3 properly. (A) The expression level of endogenous SRC-3 in HeLa cells is examined by immunofluorescence. Two channels are imaged in a single plane using a 40×/0.90 NA objective: channel 0 (DAPI) and channel 1 (SRC-3) and the resulting cell population morphologically filtered as in Fig. 1. Two galleries featuring low- and high-expressing cells are presented. A histogram is presented that demonstrates the broad range of SRC-3 immunofluorescence with a maximum fluorescence of ~220,000. (B) HeLa cells transiently expressing GFP-SRC-3 and examined for total SRC-3 (immunofluorescence) and exogenous SRC-3 expression are presented. Gallery I demonstrates the lower range of SRC-3 expression. Gallery II demonstrates the upper range of SRC-3 expression. Note the appearance of GFP-SRC-3 globules (or foci, aggregates, etc.) in mid to high SRC-3 expressing cells. To remove cells overexpressing GFP-SRC-3, the upper limit of total expression is set to three times the maximum expression found in mock-transfected cells. The corresponding maximum GFP-SRC-3 fluorescence is identified and used as a custom filter for cells transiently expressing GFP-SRC-3 and are not immunolabeled. (C) A GFP-SRC-3 expression histogram after morphological and expression filtering and a representative image gallery of HeLa cells transiently expressing GFP-SRC-3 are presented. Note the absence of subnuclear GFP-SRC-3 globules.

changes, and maintenance of the male phenotype. Testosterone mediates these functions through its receptor, AR. As noted earlier, AR resides mainly in the cytoplasm in the absence of ligand associated with heat shock proteins (HSPs). Upon agonist binding to AR, HSPs are shed, homodimerization occurs, and the receptor is phosphorylated and translocates into the nucleus. Once inside the nucleus, AR becomes organized into discrete, but unstable foci based on live cell photobleaching experiments. Activated AR then binds androgen response elements and regulates transcription through the recruitment to the promoter of transcriptional coregulators and basal transcriptional machinery (Gao *et al*., 2005). Interestingly, AR antagonists also cause nuclear translocation but without the accompanying subnuclear hyperspeckled distribution and transcriptional activity, indicating that translocation and hyperspeckling events are separable from transcription. Disruption of AR regulation has a major role in human disease (Gao *et al*., 2005; Marcelli *et al*., 2006). Mutations in AR are known to cause androgen insensitivity syndrome (AIS), which can result in a genetic male appearing phenotypically female. AR regulation of transcription also plays an important role in prostate cancer, which kills ~30,000 American men each year, second only to lung cancer. Although not causative, prostate cancer growth depends on improper regulation of AR signaling. The aberrant regulation is thought to occur by AR overexpression, AR mutations, and/or changes in AR phosphorylation (Eder *et al*., 2001; Edwards and Bartlett, 2005). The high-throughput microscopy approach allows for the rapid determination of the subcellular distribution of the hundreds of AR mutants found in association with either prostate cancer or AIS in response to large libraries of chemical compounds. This has the potential to further define mutant molecular phenotypes and identify new compounds to regulate AR activity.

Protein Translocation and Nuclear Variance Assays

Experimental Setup

Cell Culture, Treatment, and Labeling. HeLa cells for AR translocation experiments are cultured, treated, and processed as described earlier with slight modifications. HeLa cells are subcultured into either 35- or 60-mm culture dishes depending on the experiment. After 24 h of growth in stripped-FBS containing media (DMEM), cells are transfected using optimized amounts of pEGFP-AR expression vector or pEGFP-AR mutant vectors and carrier DNA (pBluescript). The cells incubate with the lipid/DNA mixture for 6 h after which the cells are subcultured again onto the

optical bottom multiwell plate at a density of 2×10^4 cells/cm^2. Higher cell densities are avoided due to the fact that it is prohibitive to accurate cytoplasmic measurements. Twenty-four hours after transfection, ligand treatments are initiated; ligands are serially diluted in stripped-dialyzed FBS containing media to generate a dose response. The length of time cells are exposed to ligand can vary depending on experimental questions, although we have found that a 2-h incubation is ideal for cytological studies of AR localization. At 2 h of 10 n*M* ligands, nuclear translocation is generally complete. Ligand treatment is stopped by washing cells with ice-cold PBS and 4% formaldehyde fixation. Fixation protocol is as described earlier.

Imaging, Data Extraction, and Data Analysis. For the DAPI channel, background fluorescence subtraction is applied, and a nucleus size range of 30 to 300 μm^2 is imposed. For the AR channel, background fluorescence subtraction is automatic, no size limit is imposed, and the extraction radius is set to ~20% greater than the average nuclear radius. In effect, only a ring of cytoplasm around the nucleus is examined. This abolishes the variation due to cells too closely spaced and errors in calculating the true cytoplasmic space for each cell.

Threshold gates similar to those described for SRC-3 are applied to each of the data sets to first extract a subpopulation of single cell objects with a biologically relevant level expression of AR. The expression level range is determined by comparative studies between transiently transfected HeLa cells and LNCaP cells, a prostate cancer-derived cell line that expresses AR. This generates the final, homogeneous population. After segmentation, a number of features are measured for each object; here we focus on two: cellular distribution and subnuclear patterns, such as the nuclear speckling associated with transcriptionally active AR (Fig. 3A).

The degree of nuclear translocation is represented by the fraction localized in nucleus (FLIN) measurement (Morelock *et al.*, 2005); the progressive reorganization of GFP-AR into a speckled pattern is captured by the nuclear variation (NVAR) measurement, which is the statistical variation in pixel brightness of the channel of interest in the nucleus. Data analysis is achieved by exporting the database files pertaining to the final gated populations to common analysis programs such as Excel and SigmaPlot/SigmaStat. Complete analysis of HTM results is beyond the scope of this chapter. Average FLIN and standard deviation among a cell population of more than thousands of cells per condition were calculated from the Excel sheet associated with extraction data.

HTM analysis is able to define distinct responses for WT AR and AR C619Y, a DNA-binding domain mutant, to various ligands. Response curves correlating the efficiency of nuclear translocation (FLIN) of

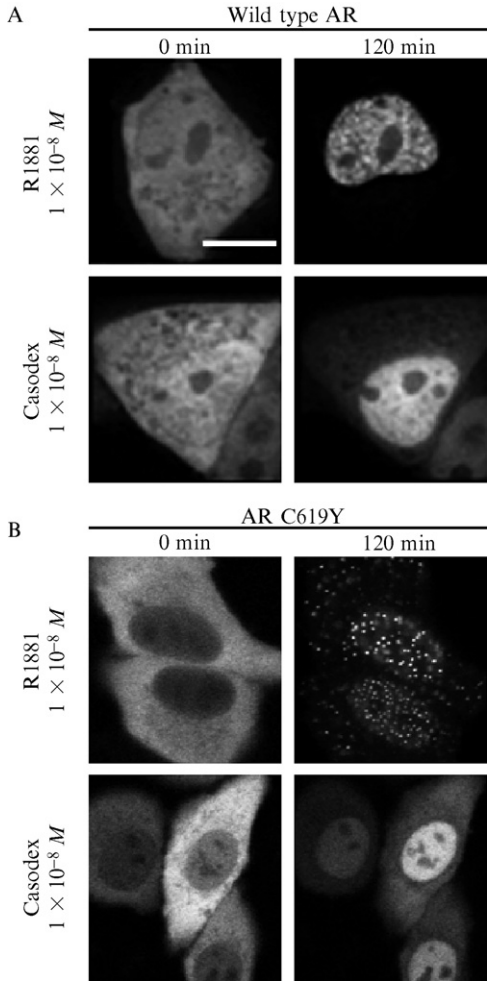

FIG. 3. High-resolution images of GFP-AR and GFP-AR C619Y. HeLa cells transiently transfected with GFP-AR (A) or GFP-AR C619Y (B) were incubated with either the synthetic AR agonist R1881 (1×10^{-8} *M*) or the AR antagonist Casodex (1×10^{-6} *M*). Cells are imaged both at 0 min (immediately before ligand addition) and at 120 min ligand treatment. R1881 induces nuclear translocation and a nuclear hyperspeckled pattern with wild-type AR. For the mutant AR C619Y, R1881 also induces nuclear translocation, but a much more dramatic focal pattern within the nucleus. For both forms of AR, Casodex is able to induce a degree of nuclear translocation, but with no hyperspeckling or foci formation.

AR-WT after administration of ligand demonstrated that nuclear translocation occurs more efficiently in response to R1881 than hydroxyflutamide (OHF), Casodex (Cas), and 17β-estradiol (E2; Figs. 3A and 4A). NVAR analysis reveals that R1881 induces the maximal degree of hyperspeckled intranuclear foci (Fig. 3A), with moderate reorganization from high levels of OHF and E2 (Fig. 4B). Importantly, AR antagonists OHF and Cas are unable to induce the same degree of nuclear speckling associated with R1881 (and are transcriptionally inactive). Highlighting the comparison between WT and mutant ARs, AR C619Y demonstrates similar ligand responses with the greatest difference being a significantly higher NVAR response to R1881, confirming the tendency of this mutant to form larger ''aggregates'' within the nucleus (Figs. 3B and 4) (Marcelli *et al.*, 2006; Nazareth *et al.*, 1999).

Estrogen Receptor

Estrogens are major promoters of cell proliferation in both normal and neoplastic breast epithelium. ERα and ERβ mediate the primary actions of estrogens at target sites around the body. These two receptors are encoded by different genes and exhibit tissue and cell-type specific expression. Augmentation of cell proliferation and an increased risk of uncontrolled cell growth and cancer is one outcome of excessive stimulation of the ERα pathway due to increased estrogen or ERα levels (Singh and Kumar, 2005). Approximately 70% of breast cancer patients are positive for elevated ERα expression at diagnosis. These patients are suitable candidates for hormone therapy that aims to block estrogen stimulation of breast cancer cells. Several antiestrogens have been developed and used as anticancer therapeutic agents and these include 4-hydroxytamoxifen (4HT) and ICI 182,780 (ICI) (Osborne *et al.*, 2000). Major goals of translational science in this arena include defining mechanisms of ligand action in regulating transcription and identifying new and tissue-specific ligands for disease treatment.

The molecular mechanisms of action for estrogens and antiestrogens at the single cell level are still being determined (Hinojos *et al.*, 2005). Single cell studies of ERα show that its subcellular distribution is predominantly nuclear, unlike AR, thus minimizing the direct usefulness prohibiting the application of cytoplasmic/nuclear fractional localization algorithms. In the absence of ligand, ERα is distributed in a diffuse nuclear pattern. The addition of ligand causes a redistribution of ERα into discrete foci. However, the nuclear redistribution of ERα does not always correlate well with transcription; for example, E2 and tamoxifen both induce subnuclear redistribution; however, in HeLa, the latter does not induce transcription. Therefore, we

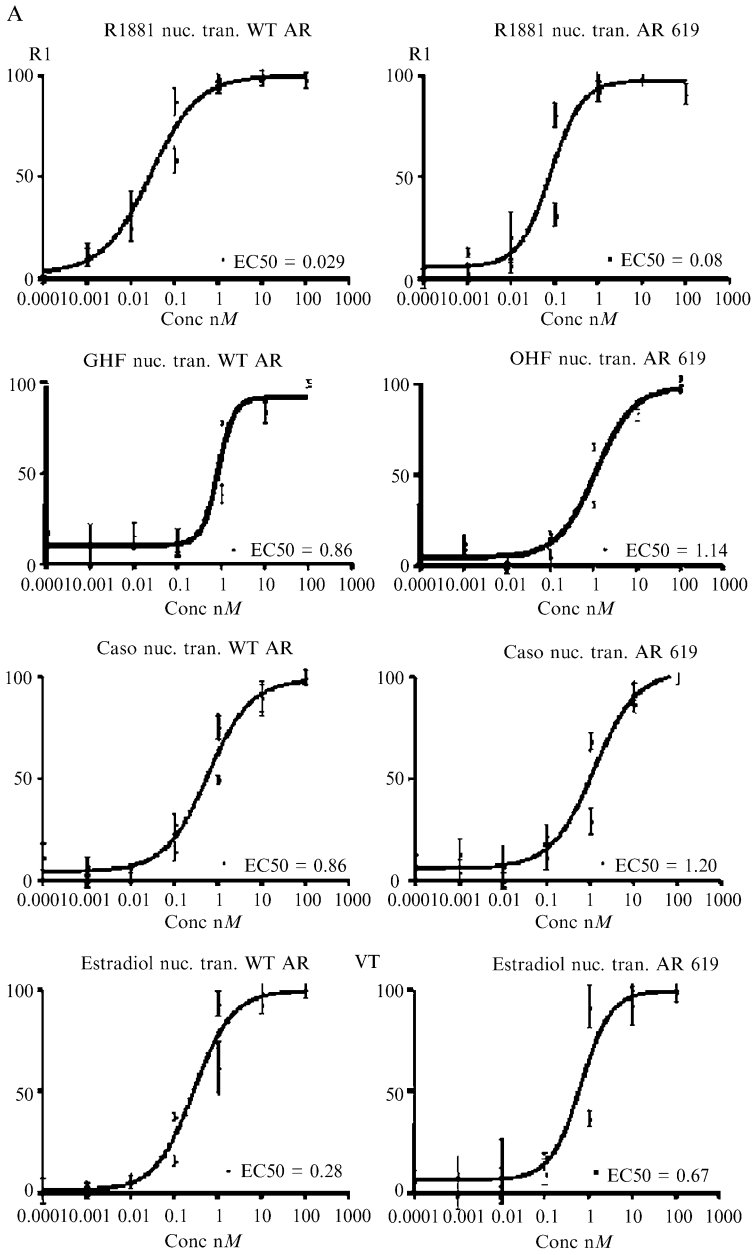
A
R1881 nuc. tran. WT AR
R1
100
50
0
EC50 = 0.029
0.00010.001 0.01 0.1 1 10 100 1000
Conc n*M*
R1881 nuc. tran. AR 619
R1
100
50
0
EC50 = 0.08
0.00010.001 0.01 0.1 1 10 100 1000
Conc n*M*
GHF nuc. tran. WT AR
100
50
0
EC50 = 0.86
0.00010.001 0.01 0.1 1 10 100 1000
Conc n*M*
OHF nuc. tran. AR 619
100
50
0
EC50 = 1.14
0.00010.001 0.01 0.1 1 10 100 1000
Conc n*M*
Caso nuc. tran. WT AR
100
50
0
EC50 = 0.86
0.00010.001 0.01 0.1 1 10 100 1000
Conc n*M*
Caso nuc. tran. AR 619
100
50
0
EC50 = 1.20
0.00010.001 0.01 0.1 1 10 100 1000
Conc n*M*
Estradiol nuc. tran. WT AR
VT
100
50
0
EC50 = 0.28
0.00010.001 0.01 0.1 1 10 100 1000
Conc n*M*
Estradiol nuc. tran. AR 619
100
50
0
EC50 = 0.67
0.0001 0.001 0.01 0.1 1 10 100 1000
Conc n*M*

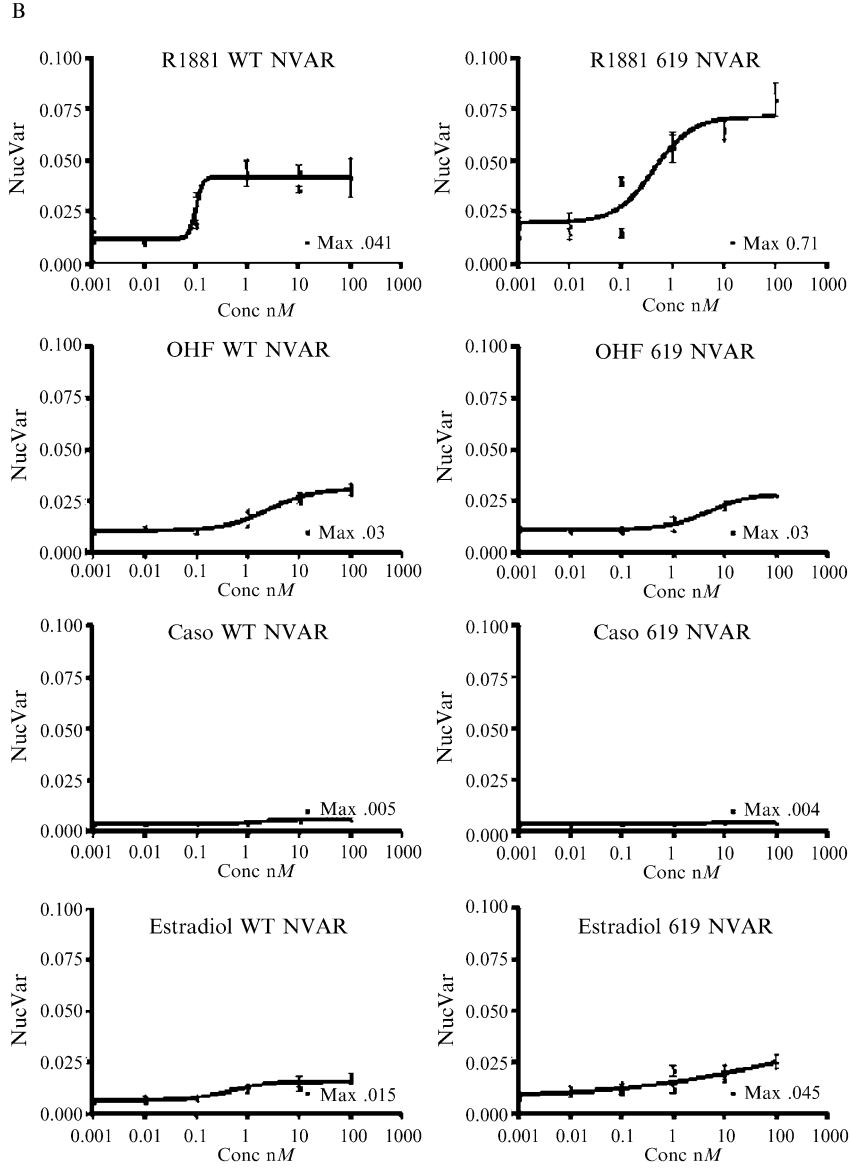

FIG. 4. Quantifying subcellular localization and patterning of AR using high-resolution HTM. HeLa cells transiently transfected with GFP-AR and GFP-AR C619Y were treated in an 11-point dose–response manner using an agonist (R1881), two antagonists (*o*-hydroxyflutamide, OHF; Casodex, Caso), and a non-AR steroid (estradiol). Experiments were done in a 96-well format and in triplicate. Nuclear translocation is quantified by using the fraction localized in nucleus (FLIN) measurement (A). Degree of nuclear speckling or foci formation is quantified using the nuclear variation (NVAR) measurement (B).

have developed a model system (PRL-HeLa cell line) that is conducive to HTM analysis in order to study ERα transcriptional properties at the single cell level. We discuss the model system and the HTM procedure for studying the chromatin remodeling/transcription function of ERα.

PRL-HeLa is a cell line specifically engineered for the single cell study of ER function (Sharp *et al.*, 2006). PRL-HeLa cells contain multiple genomic integrations of a replicated prolactin (PRL) promoter/enhancer. The multiple integrations (PRL array) are spatially confined and are visualized by the accumulation of fluorescently tagged ERα, coregulators and modified histones, and DNA FISH. The promoter/enhancers within the PRL array controls the expression of a fluorescent reporter protein targeted to cytoplasmic peroxisomes (dsRED2-Serine-Lysine-Leucine [SKL]). Addition of ERα agonist (17β-estradiol, E2) causes a rapid (within minutes) visible decondensation of the array relative to no ligand; further, antiestrogens ICI or 4HT induce a marked condensation. Importantly, the chromatin condensation/decondensation is a direct reflection of ERα-dependent coregulator recruitment and histone modification, integral features of the generally accepted model of NR regulation of transcription. Reflecting the physiological significance of the cell line and in further accord with the model of NR function, large arrays (E2-treated cells) have more (>3-fold) dsRED2-SKL transcripts at the array relative to no ligand, whereas small arrays (ICI- or 4HT-treated cells) are transcriptionally repressed (>10 fold reduction) relative to no ligand. It follows that array size in this cell line expressing ERα is an indicator of receptor transcription functionality in response to estrogenic or antiestrogenic ligand. In this manner, PRL-HeLa affords the ability to measure multiple aspects of ERα transcriptional function by HTM that is impossible in conventional cell lines.

Foci Identification and Chromatin Remodeling Assay

Experimental Setup

Cell Culture, Treatment, and Labeling. PRL-HeLa cells are cultured, treated, and processed as described earlier. Specifically, the cells are seeded onto coverslips at a density of 1–1.25 $\times$ 10^5 cells/cm^2. After 48 h in hormone-free media, cells are transiently transfected with pEGFP-ERα expression vector and carrier DNA (pBluescript) using Transfectin (Bio-Rad). The carrier to test vector DNA amount ratio is 1:1 and the lipid to DNA ratio is 2:1. Cell incubation with the DNA and transfection reagent

typically occurs overnight in hormone and phenol red-free media (DMEM). Replacing the media with prewarmed ligand containing media ends the transfection. Ligand incubation occurs for 2 h and is ended by rinsing with ice-cold PBS and fixation (see General Methods).

Imaging, Data Extraction and Filtering, and Data Analysis. Imaging of PRL-HeLa transiently expressing pEGFP-ERα is performed using the high numerical aperture 40×, 0.9 NA objective. Exposure time for pEGFP-ERα is ~2 s. A single Z section is imaged for DAPI and GFP. To maximize the number of arrays imaged, the Z section for pEGFP-ERα is offset 1 μm from the DAPI focal plane. Depending on transfection efficiency, up to ~100 fields per coverslip are imaged to obtain an unfiltered cell population of at least 5000 cells. The aggregate algorithm is automatically applied to the unfiltered cell population to identify and quantify the pEGFP–ERα foci. The aggregate identification parameters are 350 (maximum foci area in pixels), 30 (object scale), and 5 (minimum peak height). These parameters were determined to be optimal for identifying arrays in cells treated with either estrogenic (large arrays) or antiestrogenic (small arrays) ligands and for excluding nonarray identified foci. To further enhance the specificity and precision of the analysis a homogeneous cell population must be generated and is visually inspected manually in subpopulation galleries for quality control.

The unfiltered cell population has a high degree of heterogeneity (GFP-ERα expression level and identified foci, cell clusters, cell cycle, etc.) (Fig. 5A). To increase the cell population homogeneity, standard morphological and custom GFP-ER expression filters are applied as described earlier. An additional filter (number of aggregates identified per cell <10) is applied in order to remove cells with a high number of nonarray foci identified by the aggregate algorithm. The resultant filtered cell subpopulation predominantly contains in-focus and correctly identified arrays (Fig. 5B) for each treatment condition ($n > 100$). In this manner, cell filtering of a morphologically diverse cell population successfully achieved generation of a homogeneous cell population suitable for analysis of PRL array size. Quantitative cell morphology data and array measurements are contained in a data base file format.

Results of the ER chromatin-remodeling assay indicate a basal array size (no ligand control) in pixels of 70.8 ± 5.3 (Fig. 5C). Treatment with E2 causes a spatial expansion of the array (112.9 ± 3.8). Treatment with antiestrogens and breast cancer drugs 4HT or ICI causes array contraction (31.0 ± 2.5 and 29.1 ± 1.7, respectively). Array size for each treatment is significantly different than control ($p < 5\times10^{-6}$). Array size and HTM

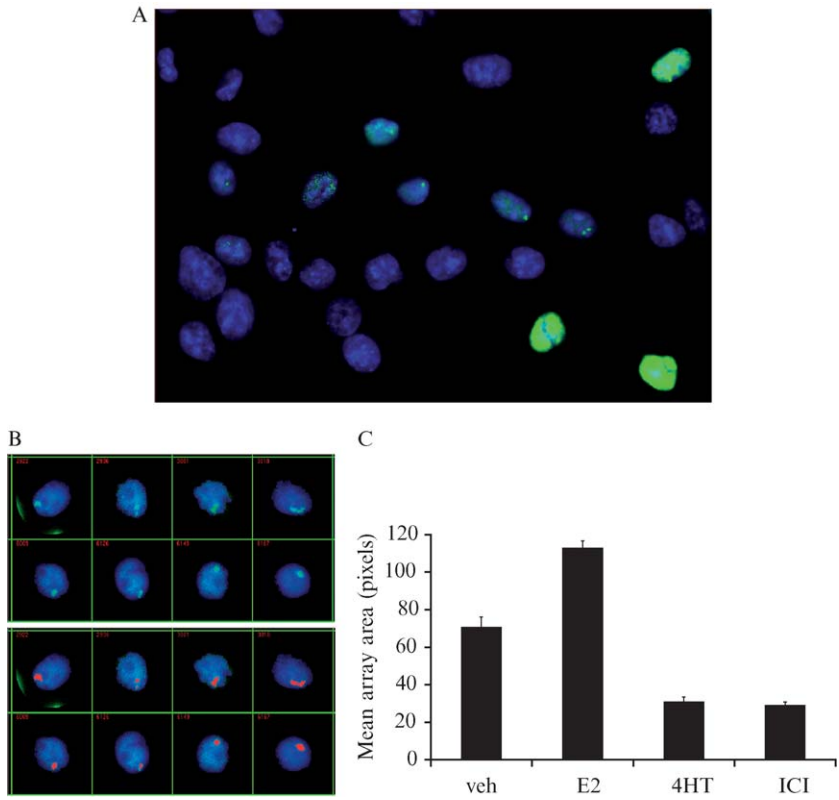

FIG. 5. Quantitative PRL array analyses. PRL-HeLa cells transiently expressing GFP-ER were treated (veh, E2, 4HT, or ICI at 10 n*M* for each ligand) for 2 h, fixed, and DAPI stained. Two channels are imaged: channel 0 (DAPI) and channel 1 (GFP-ER). (A) A representative field of E2-treated cell images is presented. Mitotic and apoptotic cells, nuclei clusters, out-of-focus cells, and cells overexpressing GFP-ER are filtered out to generate the final cell subpopulation to be analyzed as described in the text (B, top row). An aggregate identification algorithm is used to identify and quantify the GFP-ER-targeted PRL array. (B, bottom row) Results of algorithm application to identify and mask (red) the PRL array. (C) Results are presented as the mean array area in pixels ($n > 100$ for each treatment) and indicate an ER ligand-dependent regulation of chromatin remodeling.

analysis are also used to rapidly generate EC_{50} and IC_{50} values for various ERα ligands (data not shown). PRL array size is a reliable indicator of ERα ligand-dependent regulation of transcription and is quantified rapidly by HTM. Thus, PRL-HeLa and HTM have successfully demonstrated the capability to quantitatively measure distinct aspects of ERα transcription function and can now be scaled to a 96-well plate format for true

high-resolution HTM screening of ER ligand effects on chromatin remodeling. To this end, we have developed a viral-based system for high-efficiency introduction of GFP-ER and a more homogeneous subcloned PRL-HeLa line, which will be highly amenable to microtiter plate analyses.

Conclusions

Realization of high-resolution HTM as a rapid analytical method for the multiplex study of protein function is fast approaching. Driving this development is the generation of model systems such as PRL-HeLa, which allows the simultaneous study of numerous aspects of ER regulation of transcription, including nuclear translocation, DNA array targeting, chromatin modeling, coregulator recruitment, and transcription readout. While strides have been made in reducing the biological heterogeneity of cell populations to be analyzed, efficient pattern recognition algorithms still require development to overcome subcellular heterogeneity and also to take additional advantage of assays that incorporate multichannel labeling. Maturation of the field will allow for the shift of HTM research from primarily reflecting feasibility studies to true large-scale screening studies. For nuclear receptors, these studies will include mechanistic approaches such as chemical and siRNA library screening interference to define critical effectors and molecular players, respectively, in the complex signaling pathway of ligand- or nonligand-based NR activation and transcription regulation.

References

Amazit, L., Alj, Y., Tyagi, R. K., Chauchereau, A., Loosfelt, H., Pichon, C., Pantel, J., Foulon-Guinchard, E., Leclerc, P., Milgrom, E., and Guiochan-Mantel, A. (2003). Subcellular localization and mechanism of nucleocytoplasmic trafficking of steroid receptor coactivator-1. *J. Biol. Chem.* **278,** 32195–32203.

Ding, G. J., Fischer, P. A., Boltz, R. C., Schmidt, J. A., Colaianne, J. J., Gough, A., Rubin, R. A., and Miller, D. K. (1998). Development and use of a high capacity fluorescence cytometric system. *J. Biol. Chem.* **273,** 28897–28905.

Eder, I. E., Culig, Z., Putz, T., Nessler-Menardi, C., Bartsch, G., and Klocker, H. (2001). Molecular biology of the androgen receptor: From molecular understanding to the clinic. *Eur. Urol.* **40,** 241–251.

Edwards, J., and Bartlett, J. M. (2005). The androgen receptor and signal-transduction pathways in hormone-refractory prostate cancer. 1. Modifications to the androgen receptor. *BJU Int.* **95,** 1320–1326.

Evans, R. M. (1988). The steroid and thyroid hormone receptor superfamily. *Science* **240,** 889–895.

Gao, W., Bohl, C. E., and Dalton, J. T. (2005). Chemistry and structural biology of androgen receptor. *Chem. Rev.* **105,** 3352–3370.

Hinojos, C. A., Sharp, Z. D., and Mancini, M. A. (2005). Molecular dynamics and nuclear receptor function. *Trends Endocrinol. Metab.* **16,** 12–18.

Kumar, R., and Thompson, E. B. (1999). The structure of the nuclear hormone receptors. *Steroids* **64,** 310–319.

Lim, C. S., Baumann, C. T., Htun, H., Xian, W., Irie, M., Smith, C. L., and Hager, G. L. (1999). Differential localization and activity of the A- and B-forms of the human progesterone receptor using green fluorescent protein chimeras. *Mol. Endocrinol.* **13,** 366–375.

Marcelli, M., Stenoien, D. L., Szafran, A. T., Simeoni, S., Agoulnik, I. U., Weigel, N. L., Moran, T., Mikic, I., Price, J. H., and Mancini, M. A. (2006). Quantifying effects of ligands on androgen receptor nuclear translocation, intranuclear dynamics, and solubility. *J. Cell. Biochem.*

McKenna, N. J., Lanz, R. B., and O'Malley, B. W. (1999). Nuclear receptor coregulators: Cellular and molecular biology. *Endocr. Rev.* **20,** 321–344.

Morelock, M. M., Hunter, E. A., Moran, T. J., Heynen, S., Laris, C., Thieleking, M., Akong, M., Mikic, I., Callaway, S., DeLeon, R. P., Goodacre, A., Zacharias, D., and Price, J. H. (2005). Statistics of assay validation in high throughput cell imaging of nuclear factor kappaB nuclear translocation. *Assay Drug Dev. Technol.* **3,** 483–499.

Nazareth, L. V., Stenoien, D. L., Bingman, W. E., 3rd, James, A. J., Wu, C., Zhang, Y., Edwards, D. P., Mancini, M., Marcelli, M., Lamb, D. J., and Weigel, N. L. (1999). A C619Y mutation in the human androgen receptor causes inactivation and mislocalization of the receptor with concomitant sequestration of SRC-1 (steroid receptor coactivator 1). *Mol. Endocrinol.* **13,** 2065–2075.

Osborne, C. K., Zhao, H., and Fuqua, S. A. (2000). Selective estrogen receptor modulators: Structure, function, and clinical use. *J. Clin. Oncol.* **18,** 3172–3186.

Perlman, Z. E., Slack, M. D., Feng, Y., Mitchison, T. J., Wu, L. F., and Altschuler, S. J. (2004). Multidimensional drug profiling by automated microscopy. *Science* **306,** 1194–1198.

Pratt, W.B, Galigniana, M. D., Morishima, Y., and Murphy, P. J. (2004). Role of molecular chaperones in steroid receptor action. *Essays Biochem.* **40,** 41–58.

Press, M. F., Xu, S. H., Wang, J. D., and Greene, G. L. (1989). Subcellular distribution of estrogen receptor and progesterone receptor with and without specific ligand. *Am. J. Pathol.* **135,** 857–864.

Sharp, Z. D., Mancini, M. G., Hinojos, C., Dai, F., Berno, V., Szafran, A., Smith, K. P., Lele, T., Ingber, D., and Mancini, M. A. (2006). Estrogen receptor-α exchange and chromatin dynamics are ligand- and domain-dependent. *J. Cell. Sci.* In press.

Singh, R. R., and Kumar, R. (2005). Steroid hormone receptor signaling in tumorigenesis. *J. Cell. Biochem.* **96,** 490–505.

Wu, R. C., Smith, C. L., and O'Malley, B. W. (2005). Transcriptional regulation by steroid receptor coactivator phosphorylation. *Endocr. Rev.* **26,** 393–399.